Clinical Investigation

Left Circumflex Coronary Artery as the Culprit Vessel

in ST-Segment-Elevation Myocardial Infarction

Diab Ghanim, MD
Fabio Kusniec, MD
Wadi Kinany, MD
Dahud Qarawani, MD
David Meerkin, MBBS
Khaled Taha, PrEng
Offer Amir, MD, FACC
Shemy Carasso, MD

The prevalence of the left circumflex coronary artery (LCx) as the culprit vessel in ST-segment-elevation myocardial infarction (STEMI) is reportedly lowest among that of the 3 main epicardial arteries, and has not been described for non-STEMI (NSTEMI) and stable angina pectoris. We sought to define the distribution of culprit arteries in these clinical presentations and suggest mechanisms for the differences.

We reviewed 189 coronary angiograms of patients with STEMI, 203 with NSTEMI, and 548 with stable angina (n=940), and compared distributions of stenotic and culprit coronary arteries (lesions prompting intervention).

Obstructive coronary lesions (≥50% narrowing) were more prevalent in the left anterior descending coronary artery (LAD) (36%–38%) and similar in the LCx and right coronary artery (RCA) (27%–29%), regardless of clinical presentation (P <0.01). In NSTEMI and stable angina, culprit vessels and total obstructive disease had the same distribution. In STEMI, however, a culprit LCx was significantly less prevalent (17%) than was total obstructive disease (27%; P <0.01), or a culprit LAD (47%) or RCA (34%) (both P <0.001). In our computed tomographic angiographic model of coronary longitudinal strain (percentage of shortening), LCx strain was only 1.5% ± 2.4%, versus 9.5% ± 2.9% for LAD strain and 10.1% ± 3.9% for RCA strain.

In STEMI, LCx plaques seem less prone to rupturing. Culprit and total disease distributions are similar in NSTEMI and angina, suggesting a different ischemic pathophysiology in these presentations. Lower LCx longitudinal strain might contribute to reduced plaque rupture in STEMI. ***(Tex Heart Inst J 2017;44(5):320-5)***

Key words: *Acute coronary syndrome/complications/diagnostic imaging; analysis of variance; coronary stenosis/complications/diagnostic imaging/physiopathology; coronary vessels/pathology; diagnostic errors/prevention & control; models, cardiovascular; plaque, atherosclerotic/pathology; retrospective studies; rupture, spontaneous; stress, mechanical*

From: *Department of Cardiology (Drs. Amir, Carasso, Ghanim, Kinany, Kusniec, Meerkin, and Qarawani, and Mr. Taha), B Padeh Medical Center, Poriya, Lower Galilee 15208; and The Faculty of Medicine in the Galilee (Drs. Amir, Carasso, Ghanim, Kusniec, and Qarawani), Bar-Ilan University, Safed 1311502; Israel*

Address for reprints: *Shemy Carasso, MD, Cardiovascular Center, Padeh Medical Center, Poriya, Lower Galilee 15208, Israel*

E-mail: *scarasso@poria.health.gov.il*

The pathogenesis of acute coronary syndromes (ACS) predominantly involves rupture of atheromatous plaque with superimposed thrombosis.[1] The distribution of culprit coronary vessels within the different clinical manifestations of coronary artery disease (CAD)—specifically stable angina pectoris (AP), non-STEMI/unstable angina pectoris (NSTEMI/UA), and ST-segment-elevation myocardial infarction (STEMI)—is unclear. Previous investigators have found inconsistent variabilities in the distribution of culprit lesions among coronary arteries in patients presenting with ACS.[2-6] Some authors have noted an underrepresentation of the left circumflex coronary artery (LCx) in STEMI.[2,3] To our knowledge, none have looked for differences in significant total atherosclerotic distribution in these patients. Therefore, our objective in this study was to define the distribution of culprit and ≥50% diseased coronary arteries in the aforementioned clinical presentations and suggest mechanisms for the differences.

Patients and Methods

Percutaneous coronary interventions (PCI) were performed in 940 consecutive patients over an 18-month period (March 2014–October 2015) in our coronary catheterization laboratory. Of these, 548 patients had stable AP, 203 had NSTEMI, and 189 had STEMI. Patient data (clinical and procedural) were prospectively collected in our departmental database and analyzed retrospectively. Outcome data (such as biomarkers of myocardial injury, left ventricular [LV] ejection fraction, and wall-motion score) were not included in our analysis, because the focus was presentation type and coronary anatomy. The study was approved by our institutional ethics board.

Coronary Angiography

Coronary angiographic projections were chosen for the visual classification of the coronary artery map in accordance with the guidelines of the American College of Cardiology/American Heart Association.[7] In STEMI and NSTEMI, we relied upon electrocardiograms (ECG)[8] or echocardiographic identification of the myocardial area at risk[9] to conclude that an artery was "culprit"; that is, the artery had at least one lesion needing acute intervention. Each decision was made and recorded by the on-site interventional cardiologist. Total CAD distribution, defined as lesions constituting ≥50% stenosis,[10] was also recorded. In patients undergoing PCI for stable AP, culprit lesions were identified and treated by the operator on-site in accordance with the extent of narrowing, as evidenced by findings on stress tests (ECG, echocardiographic, or nuclear) or fractional flow reserve measurements.

Coronary Tree Shortening Model

Earlier investigators have correlated plaque vulnerability to vessel deformation (circumferential, and shear strains),[11-13] so we attempted to evaluate longitudinal coronary strain and its relationship to culprit-vessel distribution. Using a coronary computed tomographic angiographic (CCTA) dataset in 14 consecutive analyses conducted to exclude coronary disease, we created a dynamic 3-dimensional coronary artery anatomic model. The study was performed on a Brilliance CT 64-channel computed tomographic scanner (Koninklijke Philips N.V.; Best, The Netherlands), with retrospective ECG gating. Coronary artery measurements were obtained by using IntelliSpace Portal 6 (Philips) reconstructed straight-line multiplanar formatting views at end-diastole and end-systole (phases 0% and 40%, respectively). Longitudinal coronary deformation along the vessel's long axis or longitudinal strain (% change in length) was calculated as follows: coronary artery length (L) was measured from the ostium to a specific identifiable landmark (side branching or an acute angulation) at least 60 mm from the ostium in end-diastole (L_{ED}) and in end-systole (L_{ES}). The percentage of shortening (longitudinal strain = $[L_{ED} - L_{ES}] / L_{ED}$) was calculated for the 3 major coronary vessels. Higher strain indicated more shortening.

Statistical Analysis

Continuous data are presented as mean ± SD and categorical data as frequencies and percentages. Distribution analysis was performed with use of χ^2 tests to compare the prevalence of the culprit artery between the 3 clinical manifestations of CAD, as appropriate. One-way analysis of variance (ANOVA) with the Tukey-Kramer post hoc test was used to compare the clinical characteristics at presentation and was combined with the Bonferroni correction to detect differences in shortening between various vessels on CCTA. A *P* value <0.05 was considered statistically significant. Analyses were performed with use of MedCalc® Statistical Software version 16.4.3 (MedCalc Software bvba; Ostend, Belgium).

Results

Table I shows the patients' demographic characteristics and medical histories. When compared with patients who had NSTEMI or stable AP, the STEMI patients were younger, more often male, and more often smokers; however, hypertension, hypercholesterolemia, and diabetes mellitus were less prevalent. There were no sig-

TABLE I. Characteristics of the 940 Patients

Variable	STEMI (n=189)	NSTEMI/UA (n=203)	Stable AP (n=548)	ANOVA *P* Value	Post hoc Significant Pairwise Comparisons
Age (yr)	61 ± 15	65 ± 13	65 ± 12	0.005	1 vs 2 1 vs 3
Male	153 (81)	145 (71)	403 (74)	0.772	NS
Smoking	73 (39)	54 (27)	147 (27)	0.004	1 vs 2 1 vs 3
Hypertension	88 (47)	134 (66)	357 (65)	<0.001	1 vs 2 1 vs 3
Hypercholesterolemia	84 (44)	114 (56)	314 (57)	0.011	1 vs 3
Diabetes mellitus	54 (29)	86 (42)	201 (37)	0.021	1 vs 2
Family history of CAD	38 (20)	33 (16)	77 (14)	0.127	NS

ANOVA = analysis of variance; AP = angina pectoris; CAD = coronary artery disease; NS = not significant; NSTEMI/UA = non-ST-segment-elevation myocardial infarction/unstable angina; STEMI = ST-segment-elevation myocardial infarction

Data are presented as mean ± SD or as number and percentage. Pairwise comparisons were made with use of the Tukey-Kramer post hoc test. *P* <0.05 was considered statistically significant.

nificant differences in characteristics between patients with NSTEMI and those with stable AP.

Coronary Artery Disease and Culprit Lesions

In all clinical presentations, coronary lesions with ≥50% narrowing were somewhat more prevalent in the left anterior descending coronary artery (LAD) (36%–38%) than in the right coronary artery (RCA) and LCx (both 27%–29%; both P <0.01) (Fig. 1 and Table II). In STEMI, a culprit LCx was significantly less prevalent (17%) than that in total CAD (27%; P <0.01) and less prevalent than a culprit LAD (47%) or RCA (34%) (both P <0.001). However, in NSTEMI and stable AP, culprit vessels and total-CAD vessels were similarly distributed. Proximal true LCx involvement as the culprit in STEMI was found in only 8.5% of lesions.

Coronary Tree Shortening Model

In the 3-dimensional CCTA model, the LAD, most of the RCA, and the distal LCx and its branches traveled along the LV longitudinal axis; conversely, the proximal-to-mid LCx ran in the atrioventricular groove along the circumferential axis of the base of the LV (Fig. 2). In the 14 cases that we reviewed, the mean LAD systolic longitudinal strain was 9.5% ± 2.9% and the mean RCA strain was 10.1% ± 3.9%, compared with 1.5% ± 2.4% for the LCx. When we applied ANOVA with the Bonferroni correction, the differences between groups were significant (P <0.001). The LCx longitudinal strain differed significantly from that of the LAD (P <0.0012; 95% confidence interval [CI]= –0.0314 to –0.105) and the RCA (P <0.001; 95% CI= –0.0544 to –0.118), whereas the LAD and RCA did not differ (P=0.7; 95% CI= –0.0589 to 0.0233). Figure 3 shows an example of CCTA coronary tree reconstruction and measurements of systolic coronary strain.

Discussion

Obstructive CAD (≥50% stenosis) was rather equally distributed among the 3 main coronary vessels regardless of clinical presentation. Whereas culprit vessels followed the same distribution in NSTEMI and stable AP, the LCx was dramatically less prevalent as the culprit in STEMI, and its proximal segment even less so. In contrast, the LAD and its branches were culprits in nearly half the instances. A similar distribution pattern of culprit vessels has been reported.[2,4] Reduced sensitiv-

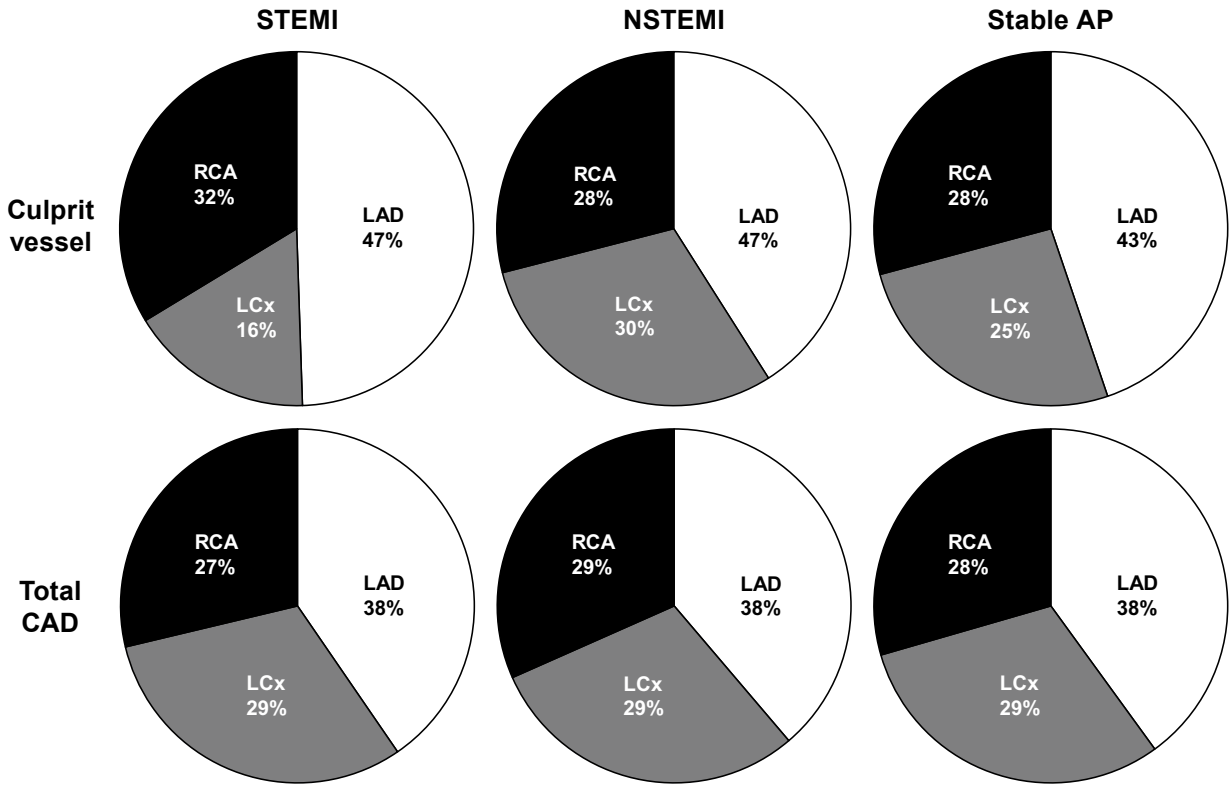

Fig. 1 *Pie charts show disease distribution among the 3 main coronary arteries in STEMI, NSTEMI, and stable AP. Note the higher prevalence of the LAD and the lower prevalence of the LCx only in STEMI, versus the more even distribution in NSTEMI, stable AP, and total obstructive CAD (narrowing, ≥50%).*

AP = angina pectoris; CAD = coronary artery disease; LAD = left anterior descending coronary artery; LCx = left circumflex coronary artery; NSTEMI = non-ST-segment-elevation myocardial infarction; RCA = right coronary artery; STEMI = ST-segment-elevation myocardial infarction

TABLE II. Relative Distribution of Coronary Lesions in the 940 Patients

Clinical Presentation (No. Patients)	Characterization of Lesions	LMCA	LAD	LCx	RCA	Ramus Intermedius	No. of Lesions	Average Lesions Per Patient
STEMI (189)	Culprit	4 (2)	89 (47)	31 (16)	61 (32)	4 (2)	189	1.0
	Total CAD	56 (4)	490 (38)	343 (27)	352 (27)	41 (3)	1,282	6.8
	All PCI	10 (4)	130 (46)	54 (19)	81 (29)	5 (2)	280	1.5
NSTEMI/UA (203)	Culprit	2 (1)	68 (40)	51 (30)	48 (28)	2 (1)	171	0.8
	Total CAD	56 (3)	583 (36)	472 (29)	462 (29)	35 (2)	1,608	7.9
	All PCI	10 (3)	127 (37)	109 (32)	87 (25)	9 (3)	342	1.7
Stable AP (548)	Culprit	9 (2)	200 (43)	116 (25)	131 (28)	11 (2)	467	0.9
	Total CAD	100 (2)	1,609 (38)	1,210 (29)	1,168 (28)	110 (3)	4,197	7.7
	All PCI	19 (2)	375 (42)	257 (29)	233 (26)	16 (2)	900	1.6

AP = angina pectoris; CAD = coronary artery disease; LAD = left anterior descending coronary artery; LCx = left circumflex coronary artery; LMCA = left main coronary artery; NSTEMI/UA = non-ST-segment-elevation myocardial infarction/unstable angina; PCI = percutaneous coronary intervention; RCA = right coronary artery; STEMI = ST-segment-elevation myocardial infarction

Culprit = lesion prompting the intervention
Total CAD = number of lesions displaying ≥50% narrowing
All PCI = all lesions treated during the index coronary intervention

Data are presented as number and percentage.

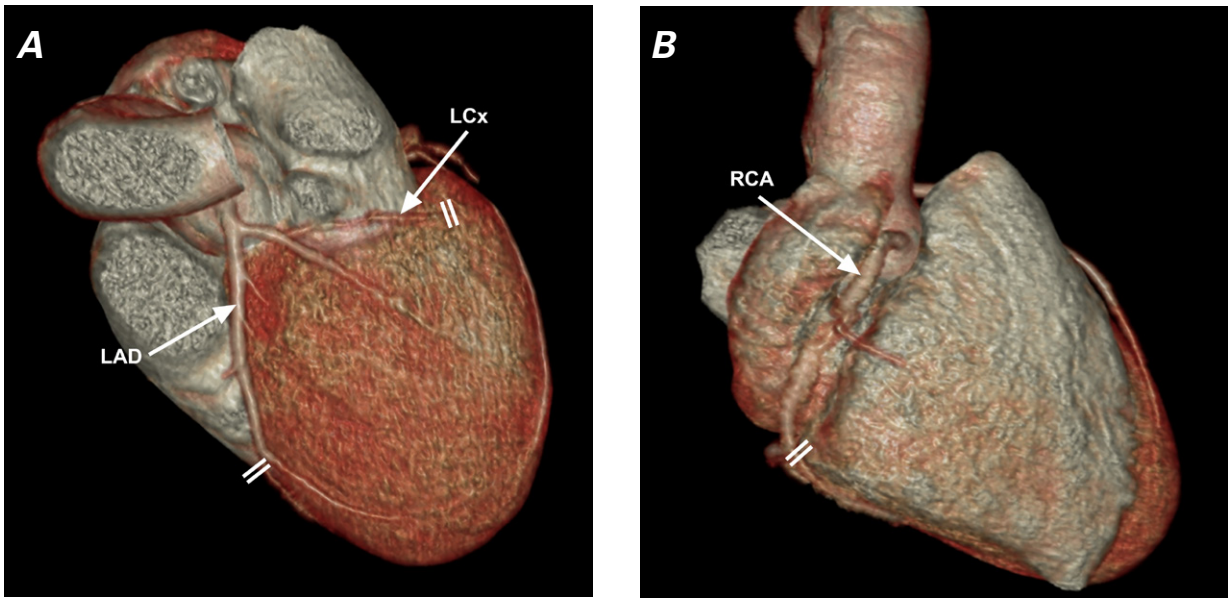

Fig. 2 *Coronary computed tomographic angiograms (3-dimensional reconstructions) show a patient's* ***A****) left coronary anatomy and* ***B****) right-dominant anatomy. Double lines denote landmarks for measuring coronary artery lengths in straight multiplanar reformatting (see Fig. 3).*

LAD = left anterior descending coronary artery; LCx = left circumflex coronary artery; RCA = right coronary artery

ity of the 12-lead ECG in detecting ischemia on the lateral and posterior walls has been suggested as a reason for less frequent diagnosis of STEMI from LCx culprit vessels and thus the decreased referral rates for primary PCI.[4,14] Anatomic variability in LCx size, branches, and caliber have also been implicated. However, these factors would not explain our having found the rather even distribution of obstructive CAD that was also very similar to that in NSTEMI and stable AP. Other investigators[3] found similar clinical characteristics (male predominance, more smoking, and less hypertension and hypercholesterolemia) and distribution of culprit vessels in a CCTA study comparing ruptured versus intact fibrous-cap plaques in ACS. Thus, the major differ-

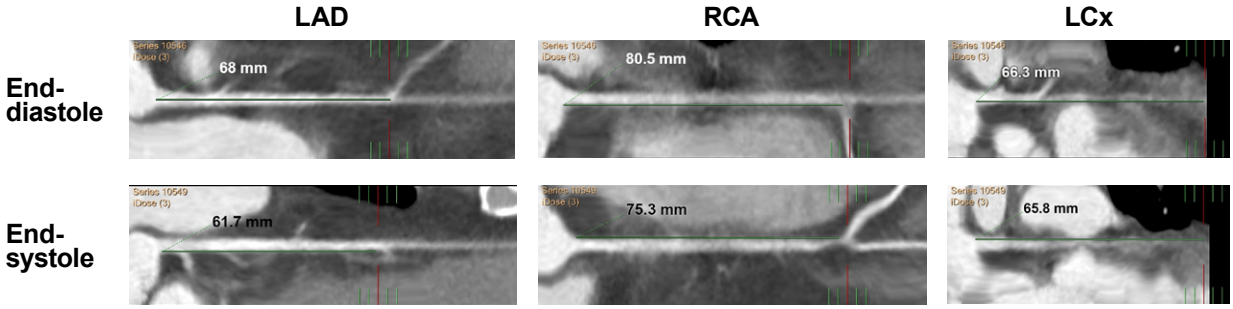

Fig. 3 *Coronary computed tomographic angiogram shows straight multiplanar reformatting of the LAD, RCA, and LCx in end-diastole and end-systole, indicating percentages of shortening of vessel length from the ostium to an identifiable landmark. Percentages of shortening (representing coronary longitudinal strain) are 9.3% in the LAD, 6.5% in the RCA, and only 1% in the LCx.*

LAD = left anterior descending coronary artery; LCx = left circumflex coronary artery; RCA = right coronary artery

ence between STEMI and NSTEMI/stable AP would probably lie in the mechanism leading to myocardial ischemia and injury.

Longitudinal Coronary Artery "Squeezing" Theory

Our remaining question concerned why plaques were less likely to rupture in the LCx than in the LAD or RCA. How did the proximal LCx differ from the LAD and RCA, and from its own distal segment and branches?

The answer may have been revealed in the 3-dimensional CCTA model. The RCA and LAD systolic shortening of approximately 10% (similar to that of the LV epicardial longitudinal-strain range)[15] differed strikingly from the 1% shortening of the proximal and mid LCx. This difference in shortening might contribute substantially to the lower prevalence of the proximal and mid LCx in STEMI.

Circumferential coronary strain is much easier to evaluate when using intravascular ultrasound. Increased circumferential strain can adversely affect plaque stability.[12] Longitudinal strain in CAD has been evaluated only in drug-eluting stents,[16] with stent-shortening in the range of 4% to 7% within stiff stents, similar to our estimation range for native coronary arteries (Fig. 3). Investigators[11] using intravascular ultrasound, 3-dimensional plaque reconstruction, and virtual histology have shown that increased wall shear stress was inversely correlated with plaque size but directly correlated with the area of the plaque's necrotic core. Thus, under repeated circumferential and longitudinal deformations, the stretching and compressing ("squeezing") of vulnerable plaques might contribute to their destabilization and eventual tearing.[11] However, because ours was not a histopathologic study, we still do not know whether this lower strain mediates the lower rates of STEMI because the LCx develops fewer vulnerable plaques, or because the vulnerable LCx plaques are less prone to rupturing.

Clinical Implications

In STEMI patients, we found fewer culprit lesions in the LCx than in the LAD and RCA, but not an absence thereof. Thus, decreased longitudinal deformation may offer a plausible partial explanation for this phenomenon and help us to understand the mechanisms of plaque rupture. The presence of a relatively well-protected coronary territory should prompt further pathophysiologic research that might yield ideas about new targets and modes of intervention.

Limitations of the Study

Identifying culprit vessels in STEMI and NSTEMI is quite straightforward on the basis of clinical presentation, ECG changes, and regional wall-motion abnormalities in preprocedural echocardiograms. In stable AP, this task is more cumbersome and requires more information derived from preadmission stress testing and fractional flow reserve functional studies during the index coronary angiography. This comparative difficulty might bias the stable-AP group toward a similar culprit and total-CAD distribution.

Conclusions

We have shown that LCx plaques appear to be less prone to rupturing in STEMI. Culprit and total-disease distribution coincide in NSTEMI and AP, suggesting a different ischemic pathophysiology in these presentations. We theorize that lower LCx longitudinal strain contributes to reduced plaque rupture in STEMI.

References

1. Alsheikh-Ali AA, Kitsios GD, Balk EM, Lau J, Ip S. The vulnerable atherosclerotic plaque: scope of the literature. Ann Intern Med 2010;153(6):387-95.
2. Antoni ML, Yiu KH, Atary JZ, Delgado V, Holman ER, van der Wall EE, et al. Distribution of culprit lesions in patients with ST-segment elevation acute myocardial infarction treat-

ed with primary percutaneous coronary intervention. Coron Artery Dis 2011;22(8):533-6.
3. Ozaki Y, Okumura M, Ismail TF, Motoyama S, Naruse H, Hattori K, et al. Coronary CT angiographic characteristics of culprit lesions in acute coronary syndromes not related to plaque rupture as defined by optical coherence tomography and angioscopy. Eur Heart J 2011;32(22):2814-23.
4. From AM, Best PJ, Lennon RJ, Rihal CS, Prasad A. Acute myocardial infarction due to left circumflex artery occlusion and significance of ST-segment elevation. Am J Cardiol 2010; 106(8):1081-5.
5. Katritsis DG, Efstathopoulos EP, Pantos J, Korovesis S, Kourlaba G, Kazantzidis S, et al. Anatomic characteristics of culprit sites in acute coronary syndromes. J Interv Cardiol 2008; 21(2):140-50.
6. Chua SK, Shyu KG, Cheng JJ, Liou JY, Lin SC, Hung HF, et al. Significance of left circumflex artery-related acute myocardial infarction without ST-T changes. Am J Emerg Med 2010;28(2):183-8.
7. PCI Writing Committee, Levine GN, Bates ER, Blankenship JC, Bailey SR, Bittl JA, et al. 2015 ACC/AHA/SCAI focused update on primary percutaneous coronary intervention for patients with ST-elevation myocardial infarction: an update of the 2011 ACCF/AHA/SCAI guideline for percutaneous coronary intervention and the 2013 ACCF/AHA guideline for the management of ST-elevation myocardial infarction: a report of the American College of Cardiology/American Heart Association Task Force on Clinical Practice Guidelines and the Society for Cardiovascular Angiography and Interventions. Catheter Cardiovasc Interv 2016;87(6):1001-19.
8. Zimetbaum PJ, Josephson ME. Use of the electrocardiogram in acute myocardial infarction. N Engl J Med 2003;348(10): 933-40.
9. Lang RM, Badano LP, Mor-Avi V, Afilalo J, Armstrong A, Ernande L, et al. Recommendations for cardiac chamber quantification by echocardiography in adults: an update from the American Society of Echocardiography and the European Association of Cardiovascular Imaging. J Am Soc Echocardiogr 2015;28(1):1-39.e14.
10. Harris PJ, Behar VS, Conley MJ, Harrell FE Jr, Lee KL, Peter RH, et al. The prognostic significance of 50% coronary stenosis in medically treated patients with coronary artery disease. Circulation 1980;62(2):240-8.
11. Corban MT, Eshtehardi P, Suo J, McDaniel MC, Timmins LH, Rassoul-Arzrumly E, et al. Combination of plaque burden, wall shear stress, and plaque phenotype has incremental value for prediction of coronary atherosclerotic plaque progression and vulnerability. Atherosclerosis 2014;232(2):271-6.
12. Veress AI, Weiss JA, Gullberg GT, Vince DG, Rabbitt RD. Strain measurement in coronary arteries using intravascular ultrasound and deformable images. J Biomech Eng 2002;124 (6):734-41.
13. Veress AI, Gullberg GT, Weiss JA. Measurement of strain in the left ventricle during diastole with cine-MRI and deformable image registration [published erratum appears in J Biomech Eng 2006;128(5):802]. J Biomech Eng 2005;127(7): 1195-207.
14. Schmitt C, Lehmann G, Schmieder S, Karch M, Neumann FJ, Schomig A. Diagnosis of acute myocardial infarction in angiographically documented occluded infarct vessel: limitations of ST-segment elevation in standard and extended ECG leads. Chest 2001;120(5):1540-6.
15. Carasso S, Biaggi P, Rakowski H, Mutlak D, Lessick J, Aronson D, et al. Velocity vector imaging: standard tissue-tracking results acquired in normals--the VVI-STRAIN study. J Am Soc Echocardiogr 2012;25(5):543-52.
16. Romaguera R, Roura G, Gomez-Lara J, Ferreiro JL, Gracida M, Teruel L, et al. Longitudinal deformation of drug-eluting stents: evaluation by multislice computed tomography. J Invasive Cardiol 2014;26(4):161-6.